18TH WORLD CONFERENCE ON EARTHQUAKE ENGINEERING
WCEE2024
MILAN

MILAN, ITALY
30TH JUNE - 5TH JULY 2024
www.wcee2024.it

STUDY OF ACTIVE CONTROL OF BASE ISOLATION SYSTEM SUBJECTED TO NEAR-FAULT PULSE GROUND MOTIONS

S. Sakamoto[1], H. Fujitani[2], Y. Mukai[2] & E. Sato[3]

[1] Kobe University, Kobe City, Japan, 221t022t@stu.kobe-u.ac.jp

[2] Kobe University, Kobe City, Japan

[3] National Research Institute for Earth Science and Disaster Resilience, Miki City, Japan

Abstract: *To achieve a high degree of continuous use of buildings in the aftermath of a large earthquake, research has been undertaken to evaluate semi-active controlled base isolation systems. However, in semi-active control experiments, under the action of the ground motion which affected JR Takatori Station during the 1995 Southern Hyogo Prefecture Earthquake, the absolute acceleration of the superstructure was greater than that achieved when using a passive base isolation system. Therefore, little effective response reduction of the semi-active control for seismic waves was observed with characteristics of near-fault pulse ground motions. This study investigates an active base isolation system that provides active control force to the base isolation structure against these near-fault pulse ground motions. To confirm the response, absolute displacement, and absolute acceleration of the superstructure, shaking table tests were conducted using a small seismic isolation specimen. The active control force was generated by AC servo motors. Seismic response analysis was also conducted to confirm the experimentally obtained results. Results show that, under the action of the observed ground motion described above, the absolute acceleration of the superstructure was reduced to about 0.6 times that measured when using a passive-base isolation system. The findings also clarified that significant response reduction of the absolute displacement and absolute acceleration of the superstructure of the base isolation system was achieved using active control under the action of other ground motions that have characteristics of near-fault pulse ground motions.*

1. Introduction

To achieve a high degree of continuous use of buildings in the aftermath of a large earthquake, research has been undertaken and knowledge has been accumulated to evaluate semi-active control of variable damping dampers installed in base isolation buildings. Fujitani et al. (2020) showed for semi-active controlled base isolation systems that, under near-fault pulse ground motion which affected JR Takatori Station during the 1995 Southern Hyogo Prefecture Earthquake, the relative displacement cannot be reduced. Moreover, the absolute acceleration of the superstructure was greater than that achieved when using a passive base isolation system. Therefore, little effective response reduction of the semi-active control for seismic waves was obtained with characteristics of near-fault pulse ground motions. This study investigates an active base isolation system that provides active control force to the base isolation system against these near-fault pulse ground motions.

Among earlier studies of active base isolation systems, Yoshida et al. (2012) presented an actual example (Laputa 2D) in which hydraulic actuators are installed in the base isolation layer. After conducting a series of studies with shaking table tests using a scaled model of a three-story base isolated building and seismic

response analysis of an actual building under Level 2 ground motions (peak ground velocity V_{max}=0.5 m/s), Yoshida et al. (2017) reported observations of an actual building using an active base isolation system. In recent years, design methods for active base isolation systems have also been proposed, as by Sato et al. (2019). Nevertheless, some room remains for study of the reduction effects of an active control system against near-fault pulse ground motions.

This study was conducted to clarify the reduction effects of an active control system under near-fault pulse ground motion and to verify the control effects using shaking table tests. In addition, the results are compared with those of earlier semi-active control experiments.

2. Calculation of Active Control Force

Calculation of the active control force follows the method described by Yoshida et al. (2012). For simplicity, a single degree of freedom system is assumed as presented in Figure 1. The equation of motion for the external seismic force is expressed in the following manner using a coordinate system relative to the ground.

$$m\ddot{x} + c\dot{x} + kx = -m\ddot{y} \tag{1}$$

In Equation (1), *m*, *c*, and *k* respectively stand for the mass, damping coefficient, and stiffness of the single-degree-of-freedom system. In addition, x, $\dot{x}$, and $\ddot{x}$ respectively represent the relative displacement, relative velocity, and relative acceleration; $\ddot{y}$ denotes ground acceleration. After transforming these into an absolute coordinate system with respect to a virtual immovable point in the air, the following equation is obtained.

$$m(\ddot{x} + \ddot{y}) + c(\dot{x} + \dot{y}) + k(x + y) = ky + c\dot{y} \tag{2}$$

In Equation (2), y and $\dot{y}$ respectively stand for the ground displacement and ground velocity. Here, the absolute response of the superstructure is controlled to be zero by application of a control force F_1 so that the right-hand side of Equation (2) is zero.

$$m(\ddot{x} + \ddot{y}) + c(\dot{x} + \dot{y}) + k(x + y) = ky + c\dot{y} + F_1 \tag{3}$$

$$F_1 = -ky - c\dot{y} \tag{4}$$

This method is designated as feedforward control (FF control) because it is a control method that takes the necessary corrective actions in advance to minimize the effects of the causes of the response. Additionally, to converge the vibration excited by the FF control error, the absolute response velocity of the structure is measured and add damping as feedback control (FB control).

$$F_2 = -c_s(\dot{x} + \dot{y}) \tag{5}$$

Therein, c_s is the viscous damping coefficient used for feedback control. From the above, the control force when FF control and FB control are used together is expressed by the following equation.

$$F = F_1 + F_2 = -ky - c\dot{y} - c_s(\dot{x} + \dot{y}) \tag{6}$$

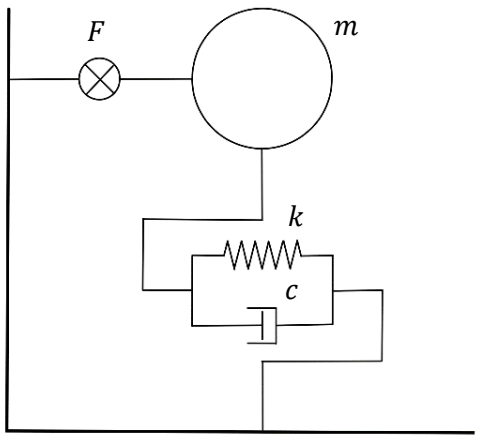

Fig. 1 Active base isolation system

3. Overview of shaking table test

3.1. Experiment system

Test specimen

The test specimen used for this study is presented in Figure 2. The base isolation layer consists of a couple of roller bearings and two coil springs. The roller bearings are fixed to the shaking table. The coil springs are pull springs that extend 800 mm from their free length and are bolted at one end to the side of the superstructure and at the other end to a sufficiently rigid steel member attached to the shaking table. The stiffness of the two coil springs is 246 N/m. The natural period is 3.0 s.

The superstructure is driven horizontally in one direction by an AC servo motor and a ball screw (30 mm lead) as a force mechanism for active control. By giving torque commands to the servo controller, the force applied to the superstructure can be controlled as desired. The maximum torque is ±7.2 Nm (equivalent thrust 1.5 kN). The maximum stroke is ±408 mm. This experiment incorporates no consideration of the similarity law with a full-scale model.

Measurement

The acceleration and displacement of the shaking table and superstructure are measured. The shaking table velocity is the derivative of the vibration table displacement. Also, the superstructure velocity is the derivative of the displacement obtained from the rotation speed of the ball screw. Velocity ($\dot{y}$) and displacement (y) of the shaking table and the absolute velocity ($\dot{x} + \dot{y}$) of the superstructure are used to calculate the active control force.

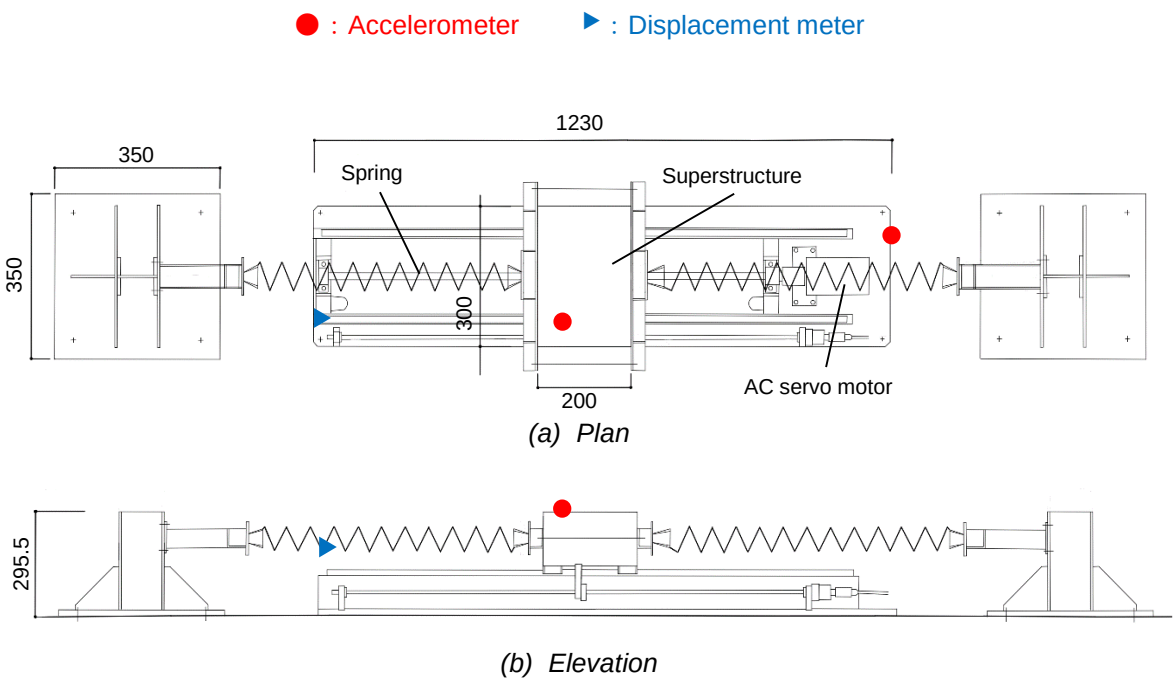

(a) Plan

(b) Elevation

Fig. 2 Experiment System (unit: mm)

3.2. Specimen characteristics

Natural frequency

The natural frequencies of the actual specimen were identified using sweep force experiments. Figure 3 shows the Bode plot obtained from the response of the specimen with a sweep wave input in the range of 0.2–5.0 Hz. The gain characteristics show good correspondence with the design value of 0.33 Hz.

Damping coefficient

The specimen is subjected to frictional forces with the roller bearing and therefore has a damping force. Damping coefficient c of the specimen is identified by conducting an experiment in which the superstructure was subjected to a sinusoidal excitation and obtaining the dynamic response factor. The obtained damping coefficient of the specimen, $c = 21.0$ Ns/m, is used for control.

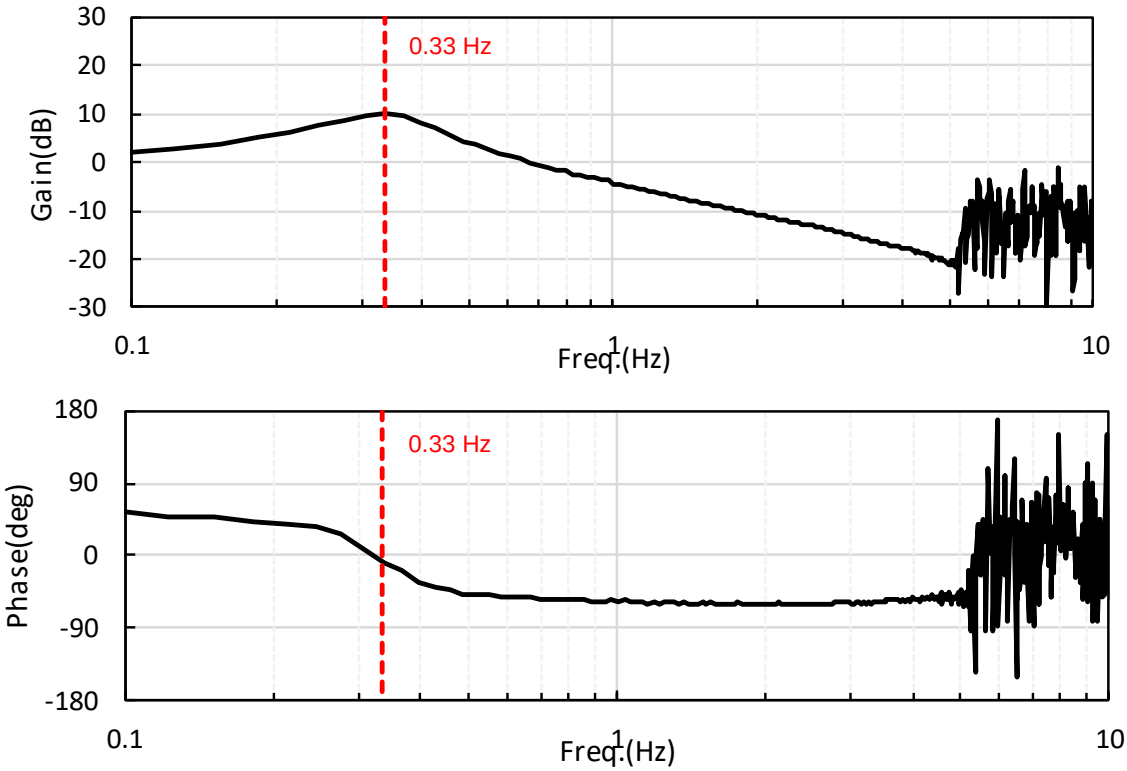

Fig. 3 Bode plot (Input, Force; Output, Structural disp.)

3.3. Input ground motion

The input ground motions are the widely used seismic waves El Centro 1940 NS and Hachinohe 1968 EW, and the pulsed seismic waves JMA Kobe 1995 NS, JR Takatori 1995 NS, Mashiki 2016 EW, and Sylmar 1994 NS. The magnitudes of the respective seismic waves are adjusted as shown in Table 1. Note that Level 2 in the table is standardized so that the maximum velocity V_{max} is 0.5 m/s. The magnification factor of input ground motion was determined from the critical amplitude of the shaking table.

Table 1 Magnification of input ground motion

El Centro 1940 NS	Level 2 (V_{max}=0.5 m/s)
Hachinohe 1968 EW	Level 2 (V_{max}=0.5 m/s)
JMA Kobe 1995 NS	100%
JR Takatori 1995 NS	70%
Mashiki 2016 EW	90%
Sylmar 1994 NS	70%

4. Verification of control effect by shaking table tests

4.1. Effects of Active Control

Test case

Using the six seismic waves shown in Section 3.3, the results of passive base isolation without control and active base isolation with active control were compared. The viscous damping coefficient c_s used for feedback was calculated as the damping constant h = 0.2. Coefficients used to calculate the active control force shown in Equation (6) are presented in Table 2.

Table 2 Coefficient for calculation of control force

k (N/m)	246
c (Ns/m)	21.0
c_s (Ns/m)	47.1

Test results

The time history waveforms of the absolute displacement and absolute acceleration of the superstructure at each seismic wave input are portrayed in Figure 4. Furthermore, Figure 5 shows a bar graph of the maximum absolute displacement and acceleration of the superstructure. The active base isolation system reduced both the absolute displacement and the absolute acceleration of the superstructure for all seismic waves used in this experiment, including pulsed seismic motion. Particularly, a marked reduction in absolute displacement is achieved.

The ratio of active control and passive seismic isolation is shown in Table 3 as the reduction ratio. The seismic wave with the smallest reduction is Hachinohe 1968 EW, which reduced the maximum absolute displacement by about 52% and the maximum absolute acceleration by about 86%. The seismic wave with the largest reduction is Sylmar 1994 NS, which reduced the maximum absolute displacement by about 17% and the maximum absolute acceleration by about 54%. However, the seismic wave with the smallest response during passive base isolation is Hachinohe 1968 EW. The largest response is Sylmar 1994 NS in this study. The response values for passive base isolation vary with the seismic wave, but the response values for active control are mutually close for all seismic waves. Consequently, the active base isolation reduces the absolute response to the same level regardless of the seismic wave characteristics.

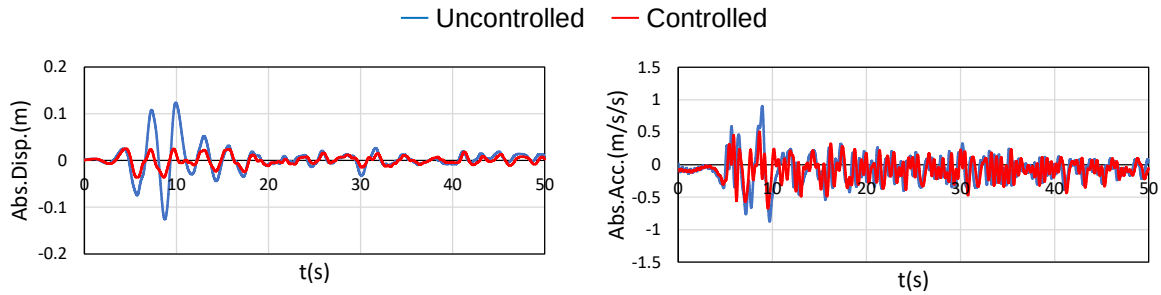

(i) Absolute displacement *(ii) Absolute acceleration*

(a) El Centro 1940 NS

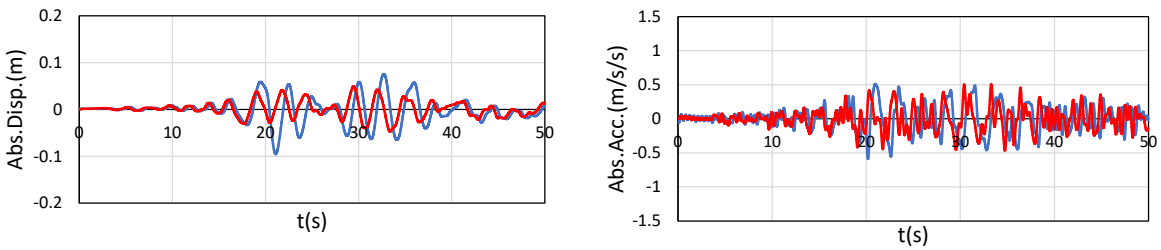

(i) Absolute displacement *(ii) Absolute acceleration*

(b) Hachinohe 1968 EW

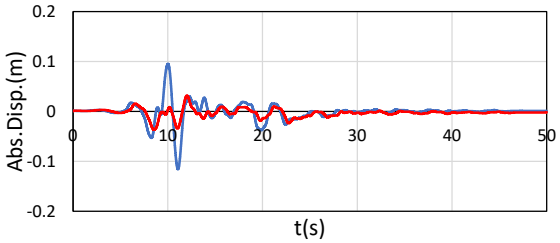

(i) Absolute displacement

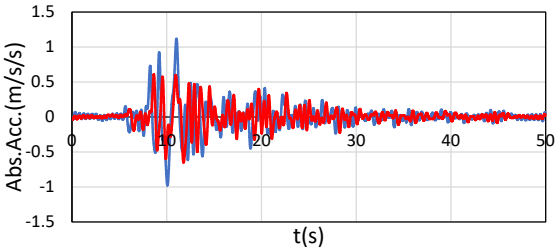

(ii) Absolute acceleration

(c) JMA Kobe 1995 NS

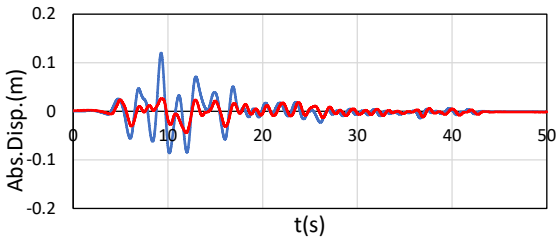

(i) Absolute displacement

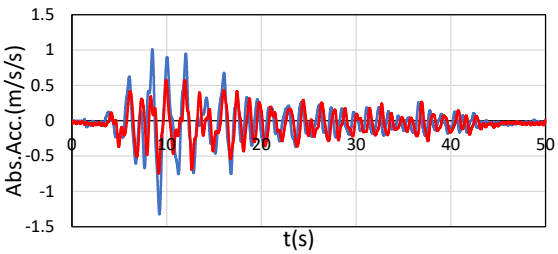

(ii) Absolute acceleration

(d) JR Takatori 1995 NS

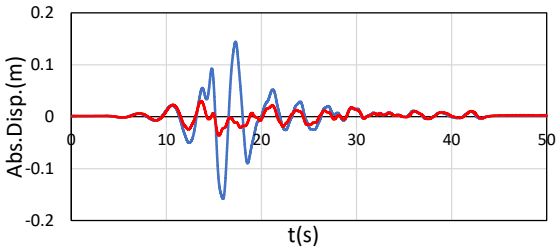

(i) Absolute displacement

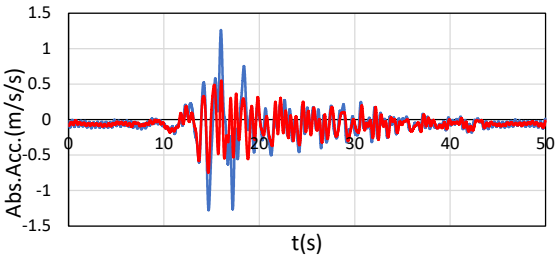

(ii) Absolute acceleration

(e) Mashiki 2016 EW

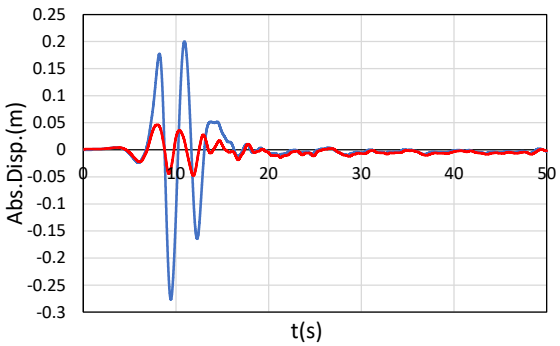

(i) Absolute displacement

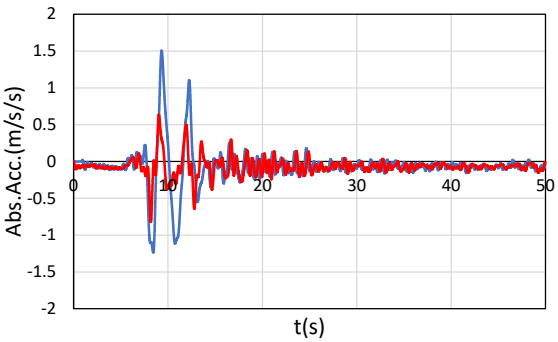

(ii) Absolute acceleration

(f) Sylmar 1994 NS

Fig. 4 Absolute response time history

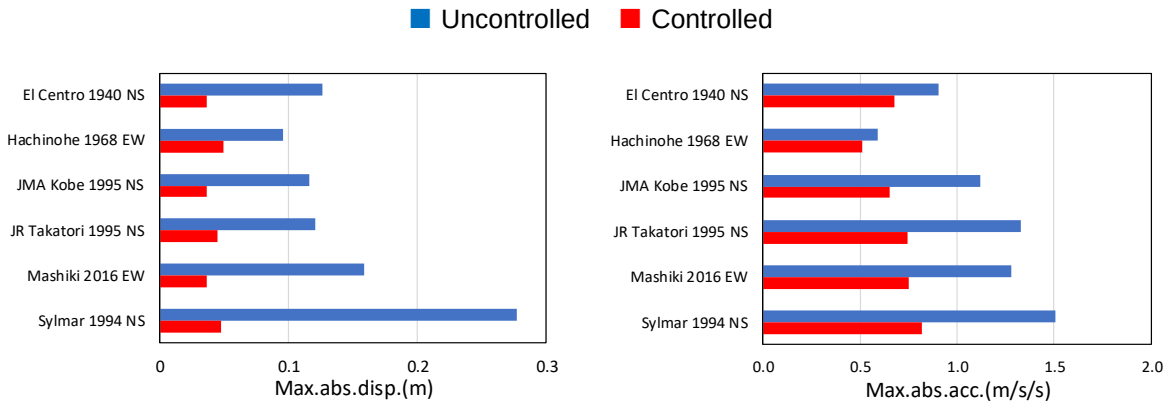

(a) Absolute displacement *(b) Absolute acceleration*

Fig. 5 Maximum response values

Table 3 Reduction rate

	El Centro 1940 NS	Hachinohe 1968 EW	JMA Kobe 1995 NS	JRTakatori 1995 NS	Mashiki 2016 EW	Sylmar 1994 NS
Max. abs. disp.	0.288	0.516	0.316	0.369	0.230	0.172
Max. abs. acc.	0.745	0.863	0.583	0.560	0.587	0.544

4.2. Comparison of reduction effect with semi-active control experiment

A comparison was made between the semi-active control experiment of a large base isolation building model reported by Fujitani et al. (2020) and this active control experiment in terms of the reduction ratio to compare their response reduction effects. Table 4 presents the specifications for the semi-active control experiment specimen. The seismic isolation specimen is a single-degree-of-freedom system. The base isolation layer consists of four roller bearings and one restoring force device (laminated rubber bearing). A magnetorheological fluid damper (MR damper), which has a damping force that varies according to the applied electric current, is installed in the base isolation layer as a semi-active control mechanism. The control method of the MR damper is state feedback optimal control (LQR). The input waves are El Centro 1940 NS (150%), JR Takatori 1995 NS (40%), and Sylmar 1994 NS (50%).

Figure 6 shows bar graphs respectively portraying the maximum relative displacement of the superstructure and the RMS value of the absolute acceleration for each seismic wave input in the semi-active control and this active control experiments. Table 5 portrays the reduction rate between the controlled and uncontrolled cases. In the semi-active control experiment, the maximum relative displacement of El Centro 1940 NS was reduced to about 50% by semi-active control, while the increase in absolute acceleration was suppressed. However, in the case of JR Takatori 1995 NS and Sylmar 1994 NS, which are near-fault pulse ground motions, little reduction is apparent in the maximum relative displacement. Particularly, the result of JR Takatori 1995 NS shows the smallest reduction of about 98% in the maximum relative displacement. The RMS absolute acceleration value increases to about 109%. In the active control experiment, however, both the relative displacement and RMS absolute acceleration values were reduced for all three waves, especially in the case of JR Takatori 1995 NS, reducing the maximum relative displacement to about 64% and the RMS absolute acceleration value to about 73%.

Table 4 Characteristics of specimen for semi-active controlled base isolation systems

Mass (ton)	14.9
Rigidity (kN/m)	44.9
Damping ratio (%)	3.58
Structural natural period (s)	3.61

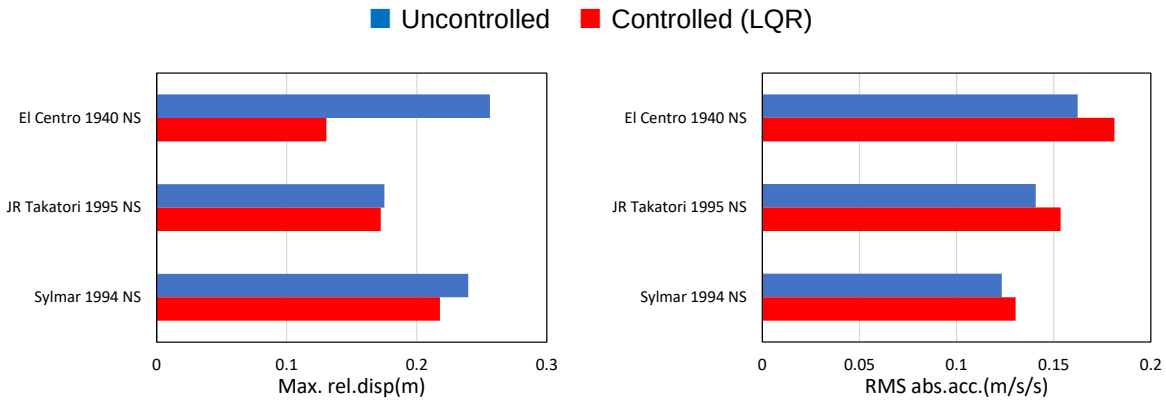

(i) Maximum relative displacement *(ii) RMS absolute acceleration*

(a) Semi-active control of base isolation

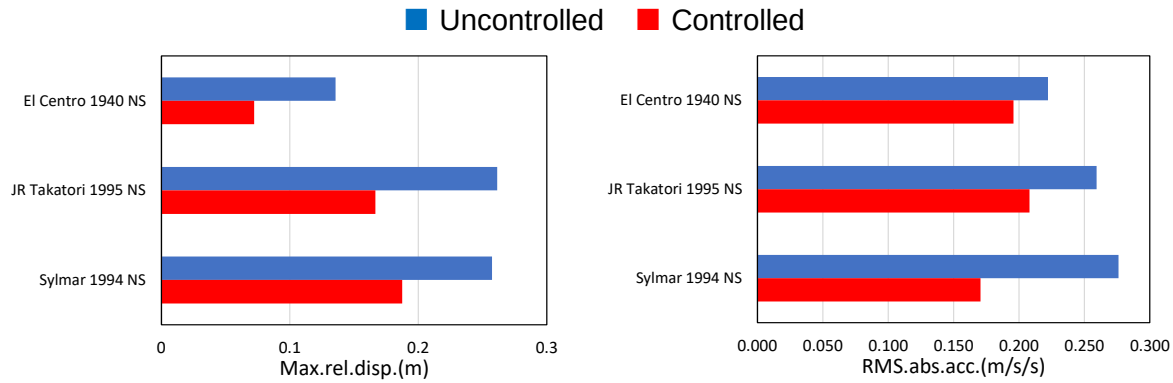

(i) Maximum relative displacement *(ii) RMS absolute acceleration*

(b) Active control of base isolation

Fig. 6 Results from two experiments

Table 5 Reduction rate

		El Centro 1940 NS	JR Takatori 1995 NS	Sylmar 1994 NS
Max. rel. disp.	Semi-active	0.509	0.984	0.909
	Active	0.532	0.637	0.728
RMS. abs. acc.	Semi-active	1.116	1.091	1.058
	Active	0.817	0.726	0.519

4.3. Effects of the Viscous Damping Coefficient Used for FB Control on Response

Test case

Next we examined the effects of the viscous damping coefficient (FB gain) c_s used for FB control, which is included in the active control force shown in Equation (6), on the response. Thirteen cases are compared, where $c_s$is expressed as a damping ratio *h* and is varied from *h*=0 to *h*=1.2 in steps of 0.1. It is noteworthy that when *h*=0, only FF control is used. The input waves are El Centro 1940 NS, JR Takatori 1995 NS, Mashiki 2016 EW, and Sylmar 1994 NS among the input waves shown in Section 3.3. For this experiment, only the FB gain is varied; FF control is performed in all cases.

Test results

Figure 7 shows the maximum absolute acceleration of the superstructure for the four input waves shown above for each FB gain case. In common with all seismic waves, there is no case in which the absolute acceleration increased significantly, even when the value of the FB gain c_s is sufficiently large. In the case of JR Takatori 1995 NS and Sylmar 1994 NS, the maximum absolute acceleration decreased concomitantly with increasing c_s. In the case of El Centro 1940 NS, the response reduction reached its peak around the value of c_s where *h*=0.5, and the maximum absolute acceleration converges to a constant value. In the case of Mashiki 2016 EW, there is less variation with the value of c_s compared to cases of other seismic waves. Although the value of c_s determines the FB control force, the effect of FB control on the response seems to exhibit different trends depending on the seismic wave characteristics.

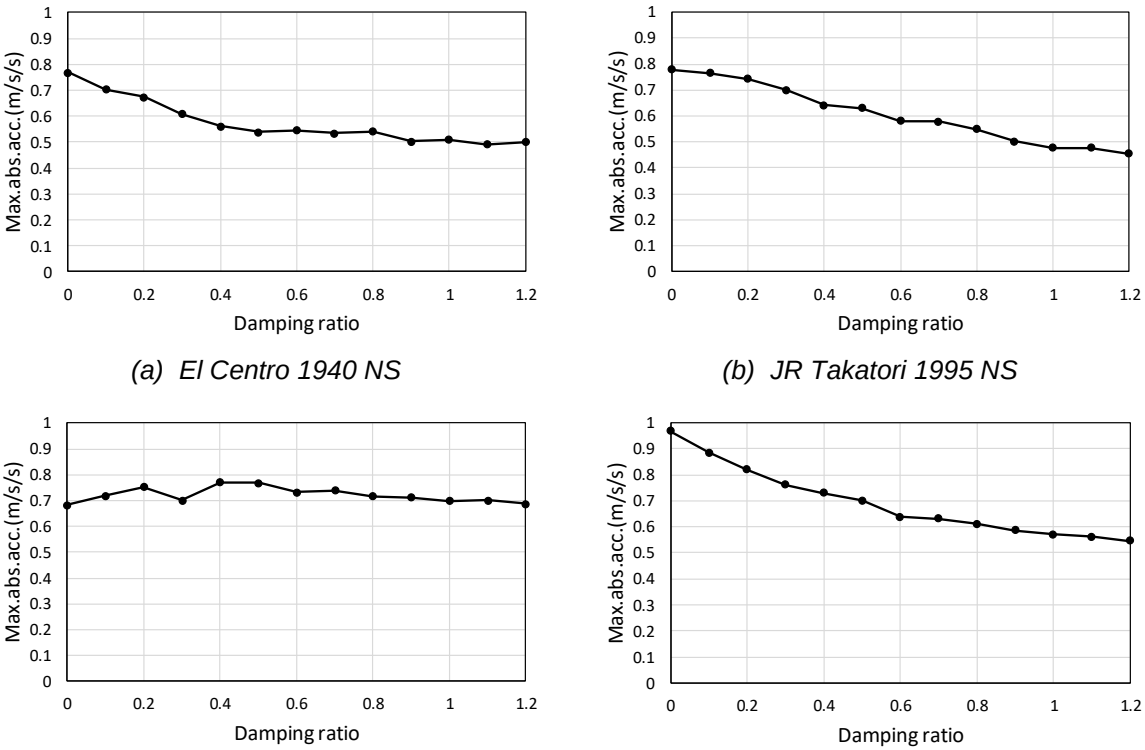

(a) El Centro 1940 NS *(b) JR Takatori 1995 NS*

(c) Mashiki 2016 EW *(d) Sylmar 1994 NS*

Fig. 7 Maximum absolute acceleration for different FB gain

5. Conclusion

This study verified the effects of active control of the base isolation system for near-fault pulse ground motion using shaking table tests with a single-degree-of-freedom test specimen. Following are the conclusions we obtained.

1. The active base isolation control reduced both the absolute displacement and absolute acceleration of the superstructure for all seismic waves used for this experiment, including near-fault pulse ground motions. Particularly, the absolute displacement was reduced significantly. Whereas the response values for passive base isolation vary with the seismic wave, the response values for control are approximately equal for all seismic waves. The active base isolation control reduces the absolute response to the same level irrespective of the seismic wave characteristics.
2. Comparison of the reduction ratios between those of the semi-active and active control experiments indicates that the active base isolation control reduced the relative displacement and RMS absolute acceleration values for two pulsed seismic waves, JR Takatori 1995 NS and Sylmar 1994 NS, for which no effective response reduction was observed with semi-active base isolation.

3. For the viscous damping coefficient (FB gain) c_s used for FB control, no case was found in which the absolute acceleration increased significantly, even when the value of c_s was sufficiently large. The trends of the absolute acceleration response with increasing c_s differed among the seismic waves we examined.

Acknowledgment

This work was supported by JSPS KAKENHI Grant Number JP22H01643.

References

Fujitani H., Mukai Y., Sato E., Johnson E.A., Christenson R., Kishida A., Ito M., Shima T., Itahara K., Iba S., Honma A. and Fukui H. (2020). Comparison of E-Defense Test Results by Five Institutes of Semi-Active Control of Base-Isolation System, *Proc. of 17th World Conference of Earthquake Engineering, Sendai, Japan: 2g-0130*

Yoshida O., Sano T., Katsumata H., Endo F., Watanabe T. and Yamanaka M. (2012). Application of Active Base Isolation System Using Absolute Vibration Control Technology, *The Japan Society of Mechanical Engineers: pp.328-339 (in Japanese)*

Yoshida O., Sano T., Katsumata H., Endo F., Watanabe T. and Yamanaka M. (2017). Application of Active Base Isolation System Using Absolute Vibration Control Technology, *Proc. of 16th World Conference of Earthquake Engineering, Santiago, Chile: Paper N° 3945*

Sato D., Chen Y., Miyamoto K. and She J. (2019). A *spectrum for estimating the maximum control force for passive-base isolated buildings with LQR control, Engineering Structures 199:* pp.109600

Nakamura Y., Uehan F., Inoue H. (1996). Waveform and its Analysis of the 1995 Hyogo-Ken-Nanbu Earthquake (II), JR Earthquake Information No. 23d, *Railway Technical Research Institute, March 1996 (in Japanese)*

National Research Institute for Earth Science and Disaster Resilience (2019) NIED K-NET, KiK-net, National Research Institute for Earth Science and Disaster Resilience, doi:10.17598/NIED.0004